15-Deoxy-$\Delta^{12,14}$-prostaglandin J_2 enhances docetaxel anti-tumor activity against A549 and H460 non-small-cell lung cancer cell lines and xenograft tumors

Suniket V. Fulzele, Abhijit Chatterjee, Madhu Sudhan Shaik[a], Tanise Jackson, Nkechi Ichite and Mandip Singh

15-Deoxy-$\Delta^{12,14}$-prostaglandin J_2 is a naturally occurring endogenous ligand for peroxisome proliferator-activated receptor-γ. The current study was aimed to determine the mechanism of anti-proliferative effect of 15-deoxy-$\Delta^{12,14}$-prostaglandin J_2 + docetaxel against A549 and H460 non-small-cell lung cancer cell lines and xenograft tumors. In-vitro cytotoxicity of 15-deoxy-$\Delta^{12,14}$-prostaglandin J_2 alone and in combination with docetaxel was studied against A549 and H460 cell lines. For in-vivo studies, female athymic *nu/nu* mice were xenografted with A549 and H460 tumors and treated with 15-deoxy-$\Delta^{12,14}$-prostaglandin J_2 (1 mg/kg/day; intraperitoneal), docetaxel (10 mg/kg; intravenous on days 14, 18 and 22) and 15-deoxy-$\Delta^{12,14}$-prostaglandin J_2 + docetaxel. Apoptosis was measured in A549 cells and tumor tissues, following various treatments. Peroxisome proliferator-activated receptor-γ, caspases, Bcl2 and p53 family proteins or their mRNA expressions were measured by Western blotting, reverse transcription-polymerase chain reaction and real-time polymerase chain reaction in A549 tumors. A possible role of a peroxisome proliferator-activated receptor-γ-independent mechanism was studied in A549 cells treated with peroxisome proliferator-activated receptor-γ antagonist, GW9662. Isobolographic analysis demonstrated synergistic interaction (combination index <1.0) between 15-deoxy-$\Delta^{12,14}$-prostaglandin J_2 and docetaxel against A549 and H460 cells *in vitro*. 15-Deoxy-$\Delta^{12,14}$-prostaglandin J_2 + docetaxel significantly reduced the tumor volume compared with control ($P<0.05$), 15-deoxy-$\Delta^{12,14}$-prostaglandin J_2 ($P<0.05$) and docetaxel ($P<0.05$, $P<0.01$) in both A549 and H460 tumors. 15-Deoxy-$\Delta^{12,14}$-prostaglandin J_2 + docetaxel showed a significant increase in apoptosis associated with inhibition of the Bcl2 and cyclin D1 expression and overexpression of caspase and p53 pathway genes. Further, enhanced expression of caspase 3 and inhibition of cyclin D1 by 15-deoxy-$\Delta^{12,14}$-prostaglandin J_2 + docetaxel was not reversed by GW9662, thus suggesting a possible peroxisome proliferator-activated receptor-γ-independent mechanism. In conclusion, 15-deoxy-$\Delta^{12,14}$-prostaglandin J_2 enhanced the anti-tumor action of docetaxel by peroxisome proliferator-activated receptor-γ-dependent and -independent mechanisms mediated by induction of apoptosis. *Anti-Cancer Drugs* 18:65–78 © 2007 Lippincott Williams & Wilkins.

Anti-Cancer Drugs 2007, **18**:65–78

Keywords: A549, Bcl2, caspase, H460, peroxisome proliferator-activated receptor-γ, 15-deoxy-$\Delta^{12,14}$-prostaglandin J_2

College of Pharmacy and Pharmaceutical Sciences, Florida A&M University, Tallahassee, Florida, [a]Current address: Barr Laboratories, Inc., Pomona, New York USA.

Correspondence to M. Singh, College of Pharmacy and Pharmaceutical Sciences, Florida A&M University, Tallahassee, FL 32307, USA.
Tel: +1 850 561 2790; fax: +1 850 599 3813;
e-mail: mandip.sachdeva@gmail.com

Sponsorship: The financial support was provided by a RCMI award (G12RR03020-11) from the NIH.

The first three authors contributed equally to this work.

Received 16 July 2006 **Revised form accepted** 23 August 2006

Introduction

Non-small-cell lung cancer (NSCLC) is the leading cause of death from malignant diseases in most developed nations. In the US and Japan, NSCLC accounts for more deaths each year than colorectal, breast and prostate carcinoma combined [1,2]. In the US alone, in 2005, there were an estimated 172 570 new cases of lung cancer and 163 510 deaths resulting from lung cancer (American Cancer Society, Facts and Figures, 2005). This accounts for the highest number of deaths among both male and female populations in any one form of cancer.

The average 5-year survival rate for localized lung cancer is 48% compared with 14.5% overall and 2.5% for metastatic lung cancer [2]. Unfortunately, only 15% of people are diagnosed at an early stage, because most lung cancers begin to grow silently without any symptoms until the cancer is in an advanced stage [3]. Thus, there is an urgent need for various new modalities for better therapeutic drugs for the prevention and treatment of lung cancer.

Several studies have been conducted in the last decade on cyclooxygenase-2 (COX-2) expression in correlation

0959-4973

with various forms of cancer. COX-2 inhibitors have been found to reduce the tumor growth rate by themselves and exert potent synergistic cytotoxic effects with anti-cancer drugs in human lung cancer cell lines [4,5]. In addition, the COX-2 inhibitor celecoxib was found to potentiate the action of chemotherapeutic drugs like docetaxel, and exert anti-proliferative and pro-apoptotic effects in a variety of cancer cell lines, including NSCLC A549, H460 and SHP77 [6,7]. The National Cancer Institute's Division of Cancer Treatment and Diagnostics has been sponsoring 20 clinical trials ranging from phase I to III in combination with celecoxib in different forms of cancer. Recent clinical trials involving patients with a history of colorectal neoplasm reported that compared with the placebo group, patients given celecoxib (200 or 400 mg, twice daily) showed a dose-dependent increase in mortality rate owing to cardiovascular problems [8]. This raised questions against the long-term use of celecoxib and COX-2 inhibitors, in general, for the treatment of cancer, and validated a search for newer treatment alternatives.

While studying COX-2 inhibitors, it was observed that celecoxib and F-L-Leu separately or in combination increased peroxisome proliferator-activated receptor (PPAR)-γ expression in methylnitrosourea-induced rat mammary tumors [9]. Similarly, overexpression of PPAR-γ in oral squamous carcinoma and NSCLC cells by sulindac sulfide has also been reported [10,11]. We recently reported that nimesulide and celecoxib in combination with docetaxel enhance PPAR-γ expression, which may contribute to the anti-tumor effect in NSCLC A549 xenograft tumors [6,12]. Therefore, it may be hypothesized that PPAR-γ provides a possible alternative target for cancer treatment. Currently, the PPAR-γ agonist pioglitazone is under National Cancer Institute supported phase IIa clinical trial for prevention of oral cancer or leukoplakia in the School of Dentistry, University of Minnesota.

PPARs are members of the nuclear hormone receptor family. They are the ligand-activated transcription factors that heterodimerize with the vitamin A derivative retinoid RXRs and bind to peroxisomal proliferator receptor response elements in the promoter region of target genes. Three major subtypes of these receptors have been described (PPAR-α, -β/δ and -γ), and they are involved in the control of lipid metabolism and homeostasis. Recently, they have been linked to the processes of cellular proliferation, differentiation and apoptosis by complex and incompletely understood mechanisms. Recent investigations have demonstrated that activation of PPAR-γ leads to growth inhibition of human prostate [13], colon [14], breast [15] and lung cancer [12] by specific mechanisms, which include induction of apoptosis and growth arrest. PPAR-γ receptors are activated by several lipophilic ligands, including long-chain polyunsaturated fatty acids and several eicosanoid derivatives that bind to the PPAR-γ receptor at micromolar concentrations. The essential fatty acids gamolenic acid, arachidonic acid, docosahexanoic acid and eicosapentaenoic acid, as well as modified oxidized lipids (9-hydroxyoctadecadienoic acid and 13-hydroxyoctadecadienoic acid) bind to and activate PPAR-γ.

15-Deoxy-$\Delta^{12,14}$-prostaglandin J_2 (15d-PGJ_2) is suggested to be the most potent endogenous ligand for the PPAR-γ receptor and the most commonly used naturally occurring PPAR-γ agonist. The prostanoid 15d-PGJ_2 is a cyclopentenone-type prostaglandin derived by dehydration of prostaglandin D_2, produced by different cell types. The cyclopentenone may alter cellular functions by multiple mechanisms. 15d-PGJ_2 has been shown to inhibit the expression of a variety of proinflammatory genes including COX-2 [14]. Some of the effects of 15d-PGJ_2 are mediated by its ability to bind and activate PPAR-γ [16,17]. However, it is also reported that 15d-PGJ_2 negatively regulates nuclear factor (NF)-κB activity owing to the two electrophilic carbonyls within its ring structure that form a covalent Michael adduct with cysteine-containing products. 15d-PGJ_2-mediated NF-κB inhibition is accompanied by sharp downregulation of NF-κB-dependent anti-apoptotic gene products, including cellular inhibition of apoptosis protein (XIAP), and FLICE-inhibitory protein (cFLIP) [14]. Although several studies have been conducted with 15d-PGJ_2 *in vitro*, no study has been conducted with 15d-PGJ_2 alone or in combination with any other drug in animal models. Thus, the current study evaluates the anti-tumor efficacy of 15d-PGJ_2 + docetaxel in advanced xenografted lung tumors in mice. The objectives of the present study are to: (1) study the enhancement of in-vitro and in-vivo anti-tumor effect of docetaxel by 15d-PGJ_2 in A549 and H460 lung tumors, and (2) study and explore the possible pathways mediating apoptosis and growth inhibition by 15d-PGJ_2 + docetaxel in advanced A549 xenograft lung tumors.

Materials and methods

Materials

Docetaxel was a gift sample from Sanofi-Aventis (Collegeville, Pennsylvania, USA). 15d-PGJ_2 and GW9662 were procured from Cayman Chemical Company (Ann Arbor, Michigan, USA). A549 and H460 cell lines were obtained from American Type Culture Collection (Rockville, Maryland, USA). Antibodies against PPAR-γ and caspase 3 were purchased from Cayman Chemical Company. Prostaglandin E_2 (PGE_2) colorimetric enzyme immunoassay kits were purchased from Assay Designs (Ann Arbor, Michigan, USA). The Dead-End Colorimetric Apoptosis Detection kit was obtained from Promega (Madison, Wisconsin, USA). Tissue culture chemicals obtained from Sigma (St Louis, Missouri, USA) were either of reagent or tissue culture grade.

In-vitro cytotoxicity studies

Cancer cell lines (A549 and H460) were plated into 96-well microtiter plates at a concentration of 10 000 cells/well and allowed to incubate overnight. Stock solution of 15d-PGJ$_2$ was prepared in dimethylsulfoxide and subsequent dilutions were made in appropriate tissue culture media. Various dilutions of 15d-PGJ$_2$ (1–20 μmol/l) were added to the cells and the plates were incubated for 72 h at 37 ± 0.2°C in a 5% CO_2-jacketed incubator. The reduction in 50% inhibitory concentration (IC_{50}) of docetaxel brought about by its combination with 15d-PGJ$_2$ was determined. The cytotoxicity was assessed by crystal violet dye uptake assay, and quantified by measuring the absorbance of the dye at a wavelength of 540 nm using an automated microquant plate reader (Biotek Instruments, Winooski, Vermont, USA) and KC3 software. The IC_{50} values were determined by plotting the log of the percentage cell kill values versus drug concentration and was used to generate isobolograms. For 50% cytotoxicity, combination index (CI) values were calculated.

$$\mathrm{CI} = (D)_1/(D_x)_1 + (D)_2/(D_x)_2 + \alpha(D)_1(D)_2/(D_x)_1(D_x)_2 \quad (1)$$

where $(D_x)_1$ is the dose of drug 1 to produce 50% cell kill alone, $(D)_1$ is the dose of drug 1 to produce 50% cell kill in combination with $(D)_2$, $(D_x)_2$ is the dose of drug 2 to produce 50% cell kill alone, $(D)_2$ is the dose of drug 2 to produce 50% cell kill with $(D)_1$ and $\alpha = 0$ for mutually exclusive or 1 for mutually non-exclusive modes of drug action.

In-vivo anti-tumor effect of 15-deoxy-$\Delta^{12,14}$-prostaglandin J$_2$, docetaxel and 15-deoxy-$\Delta^{12,14}$-prostaglandin J$_2$ + docetaxel against A549 and H460 lung tumors

Female *nu/nu* mice (6 weeks old; Harlan, Indianapolis, Indiana, USA) were preselected for subcutaneous A549 and H460 tumors, and xenografts were transplanted by subcutaneous administration of 5×10^6 A549 and H460 cells, respectively, in the right hind leg [12]. The protocol for in-vivo experiments with nude mice was approved by the Animal Care and Use Committee, Florida A&M University, Tallahassee, Florida, USA. Fourteen days after tumor implantation, the mice were treated with 15d-PGJ$_2$ (1 mg/kg/day, intraperitoneal) until the end of the study (28 days). Docetaxel (10 mg/kg) was given intravenously on days 14, 18 and 22 after tumor implantation. The combination treatment group was given 15d-PGJ$_2$ and docetaxel in the same way as administered for their respective individual treatments. The control mice were administered vehicle only. Tumor dimensions were measured twice weekly using a linear caliper and the tumor volume was calculated using the equation $V\ (\mathrm{mm}^3) = a \times b^2/2$, where a is the largest diameter and b is the smallest diameter. The mice were fed with food and water *ad libitum*.

Terminal deoxynucleotidyl transferase-mediated deoxyuridine triphosphate-biotin nick-end-labeling assay of A549 cells and xenograft tumors treated with 15-deoxy-$\Delta^{12,14}$-prostaglandin J$_2$ + docetaxel

To detect apoptotic cells, the ApoTag Red In situ Apoptosis detection kit (Chemicon International, Temecula, California, USA) was used. Cells were plated at a density of 1×10^6 cells/well in six-well plates and incubated overnight. Cells were treated with docetaxel (0.01 μmol/l), a 15d-PGJ$_2$ (10 μmol/l) or combination of docetaxel (0.01 μmol/l) and 15d-PGJ$_2$ (10 μmol/l). The control cells were left untreated. After 72 h, cells were fixed in 4% paraformaldehyde and mounted onto slides using Cytospin (Shandon, Pittsburgh, Pennsylvania, USA). Equilibration buffer was added to slides and incubated for 10 min followed by incubation in working strength terminal deoxynucleotidyl transferase (TdT) enzyme at 37°C for 1 h. The slides were incubated in stop/wash buffer for 10 min at room temperature. Working strength anti-digoxinenin conjugate (rhodamine) was added to each slide for 30 min incubation at room temperature. Slides were viewed using a fluorescent microscope. To quantify the apoptotic cells from TdT-mediated deoxyuridine triphosphate-biotin nick-end labeling (TUNEL) assay, 100 cells from six random microscopic fields were counted. One-way analysis of variance followed by the post-hoc Tukey test was used for statistical analysis to compare control and treated groups.

For A549 xenograft tumors, the DeadEnd colorimetric apoptosis detection system (Promega) was used to detect apoptosis at 28 days after tumor implantation. The tumor tissue samples collected at the end of the study were frozen in a cryomatrix and sectioned in a cryotome (Shandon Cryotome 0620; Thermo Shandon, Pittsburgh, Pennsylvania, USA). The tumor tissue cryo-sections were washed in phosphate-buffered saline (PBS) and then fixed in 4% paraformaldehyde solution before incubation in 20 μg/ml proteinase K for 10 min. The sections were washed in PBS and incubated with TdT enzyme in a humidified chamber at 37°C for 60 min for incorporation of biotinylated nucleotides at the 3′-OH DNA ends. After endogenous peroxidase quenching, horseradish peroxidase-labeled streptavidin was used to bind the biotinylated nucleotides, which were finally detected using hydrogen peroxide and stable chromogen 3,3′-diaminobenzidine. Slides were observed with an Olympus BX40 light microscope equipped with a computer-controlled digital camera (QImaging, Burnaby, British Columbia, Canada) and imaging software.

Determination of prostaglandin E$_2$ levels in A549 tumor tissues

The tumor tissue samples were homogenized in 70% ethanol and 30% 0.1 mol/l sodium phosphate (pH 4.0), and incubated on wet ice for 30 min. The samples were centrifuged and the supernatants were collected. A known

volume of supernatant (typically 250 µl) was dried under nitrogen, resuspended in assay buffer and analyzed for PGE_2 using a colorimetric enzyme immunoassay kit following the manufacturer's protocol (Assay Designs).

Western blotting of A549 tumor tissues

Tumor tissues harvested at 28 days after tumor implantation from control, 15d-PGJ_2, docetaxel and 15d-PGJ_2 + docetaxel-treated mice were cut into small pieces and homogenized in PBS. The homogenate was centrifuged at high speed for 10 min to sediment the tissue fragments followed by the addition of lysis buffer (25 mmol/l *N*-2-hydroxyl piperazine-*N*′-2-ehane sulfonic acid, Triton-X 0.1%, NaCl 300 mmol/l, β-glycerophosphate 20 mmol/l, $MgCl_2$ 1.5 mmol/l, ethylenediaminetetraacetic acid 0.2 mmol/l, dithiothreitol 25 mmol/l) with protease inhibitors (sodium orthovanadate 4 mmol/l, sodium fluoride 400 mmol/l, benzamidine 20 mmol/l, leupeptin 2 µg/ml, aprotinine 4 µg/ml, phenylmethylsulfonyl fluoride 500 µmol/l). Samples were vortexed, incubated on ice for 30 min, centrifuged again and the supernatants were stored at −80°C. For Western blotting, equal amounts of supernatant protein (30 µg) from the control and different treatments were denatured by boiling for 5 min in sodium dodecyl sulfate sample buffer, separated by 8% sodium dodecyl sulfate–polyacrylamide gel electrophoresis and transferred to nitrocellulose membranes for immunoblotting. The membranes were blocked with 5% skim milk in Tris–buffered saline with Tween 20 [10 mmol/l Tris–HCl (pH 7.6), 150 mmol/l NaCl, 0.5% Tween 20] and probed with PPAR-γ and caspase-3 antibodies (1 : 500). Bound antibodies were revealed with horseradish peroxidase-conjugated secondary antibodies (1 : 2000) using SuperSignal West pico chemiluminescent solution (Pierce, Rockford, Illinois, USA).

Real-time polymerase chain reaction analysis of gene expression

The tumor tissues collected at the end of the study (28 days after tumor implantation) were processed to isolate total RNA using the RNeasy Protect Mini kit (Qiagen Valencia, California, USA). Total RNA was quantified and 100 ng of the RNA was reverse transcribed using TaqMan reverse transcription reagents at 48°C for 30 min. The cDNA was then amplified using TaqMan Universal polymerase chain reaction (PCR) master mix and Assay on Demand primer probe sets for PPAR-γ, caspase-3, caspase 8, caspase 9, cyclin D1 and internal control 18S RNA in a real-time PCR system 7300 (Applied Biosystems, Foster City, California, USA). Data were collected at the end of 40 cycles and analyzed using the RQ Study software v1.3 (Applied Biosystems).

Reverse transcription-polymerase chain reaction of the tumor tissues

Reverse transcription was performed with Reaction Ready First Strand cDNA Synthesis Kit (Super Array, Frederick, Maryland, USA) according to the manufacturer's protocol. The PCR amplification of the first strand cDNA was performed using the ReactionReady Hot Start 'Sweet' PCR master mix and primer sets from human caspase, Bcl2 and p53 gene families following the conditions: (94°C, 15 min) followed by 30 cycles of 94, 55 and 72°C (30 s each). The PCR products were separated in a 2% agarose gel and the band intensities were normalized with respect to glyceraldehyde-3-phosphate dehydrogenase using Image J 1.33u Software (National Institute of Health, Bethesda, Maryland, USA).

In-vitro studies with A549 cells to determine involvement of peroxisome proliferator-activated receptor-γ

One million A549 cells in 10 ml media (with or without 20 µmol/l GW9662) were plated in 25-cm^2 flasks and incubated overnight. Subsequently, they were treated with 15dPGJ_2 (10 µmol/l), docetaxel (0.01 µmol/l) and 15dPGJ_2 + docetaxel (10 + 0.01 µmol/l) for 24 h. Finally, the total RNA was isolated; reverse transcribed and PPAR-γ, caspase-3 and cyclin D1 measured by real-time PCR.

Results

Enhancement of the in-vitro cytotoxicity of docetaxel by 15-deoxy-$\Delta^{12,14}$-prostaglandin J_2 in A549 and H460 cells

In A549 cells, IC_{50} values of 15d-PGJ_2 and docetaxel were 16.68 ± 0.82 and 0.025 ± 0.003 µmol/l, respectively. 15-dPGJ_2 enhanced the docetaxel cytotoxicity in a synergistic manner at 6, 10 and 12 µg/ml, and produced an additive effect at 15 µg/ml (Table 1). The concentration of 15d-PGJ_2 employed for enhancing the docetaxel activity was below its IC_{50} value (16.68 µmol/l). Similarly, in H460 cells, IC_{50} values of 15d-PGJ_2 and docetaxel were 19.21 ± 1.22 and 0.014 ± 0.005 µmol/l, respectively. 15d-PGJ_2 synergistically reduced the IC_{50} value of docetaxel at concentrations of 6, 10, 12 and 15 µmol/l (Table 1). The concentration of 15d-PGJ_2 employed for enhancing the docetaxel activity was again below its IC_{50} value (19.21 µmol/l) against H460 cells. It is evident from isobolographic analysis shown in Table 1, that 15d-PGJ_2 at different concentrations showed synergism to additive effect when combined with docetaxel against both A549 and H460 cells.

15-Deoxy-$\Delta^{12,14}$-prostaglandin J_2 enhances docetaxel activity against A549 and H460 tumor xenografts

Figures 1 and 2 show the tumor volume–time data profiles following the administration of vehicle control, 15d-PGJ_2, docetaxel and 15d-PGJ_2 + docetaxel in mice xenografted with A549 and H460 tumors, respectively. It is evident from Fig. 1 that in A549 tumors, 15d-PGJ_2 + docetaxel produced potent anti-tumor effect as compared with 15d-PGJ_2 or docetaxel treatment alone. At 28 days after tumor implantation, the tumor volumes were found to be 1849 ± 284.6, 1529 ± 243.2,

Table 1 Effect of 15d-PGJ$_2$ on the in-vitro cytotoxicity of docetaxel against lung cancer cell lines A549 and H460

Cell line	IC_{50} of 15d-PGJ$_2$ alone (μmol/l)	IC_{50} of docetaxel alone (μmol/l)	Drug combinations	Reduced IC_{50} of docetaxel	Reduction (%)	CI
A549	16.68 ± 0.82	0.025 ± 0.003	DOC + 15d-PGJ$_2$ 6 μmol/l	0.0025 ± 0.002	90.0	0.447
			DOC + 15d-PGJ$_2$ 10 μmol/l	0.0018 ± 0.001	92.8	0.671
			DOC + 15d-PGJ$_2$ 12 μmol/l	0.0017 ± 0.001	93.2	0.787
			DOC + 15d-PGJ$_2$ 15 μmol/l	0.0011 ± 0.001	95.6	0.943
H460	19.21 ± 1.22	0.014 ± 0.005	DOC + 15d-PGJ$_2$ 6 μmol/l	0.0023 ± 0.001	83.5	0.476
			DOC + 15d-PGJ$_2$ 10 μmol/l	0.0022 ± 0.001	84.2	0.677
			DOC + 15d-PGJ$_2$ 12 μmol/l	0.0014 ± 0.001	90.0	0.738
			DOC + 15d-PGJ$_2$ 15 μmol/l	0.0013 ± 0.002	90.7	0.887

The human lung cancer cell lines A549 (adenocarcinoma) and H460 (large-cell carcinoma) were obtained from American Type Culture Collection (Rockville, Maryland, USA). 15d-PGJ$_2$ was used at 6, 10, 12 and 15 μmol/l to study the effect on IC_{50} of docetaxel. Variable ratios of drug concentrations were used to determine the in-vitro cytotoxicity data and mutually non-exclusive equations were used to determine the CI. The CI values represent the mean of three experiments. CI > 1.3: antagonism; CI 1.1–1.3: moderate antagonism; CI 0.9–1.1: additive effect; CI 0.8–0.9: slight synergism; CI 0.6–0.8: moderate synergism; CI 0.4–0.6: synergism; CI 0.2–0.4: strong synergism.
IC_{50}, 50% inhibitory concentration; DOC, docetaxel; 15d-PGJ$_2$, 15-deoxy-$\Delta^{12,14}$-prostaglandin J$_2$; CI, combination index.

Fig. 1

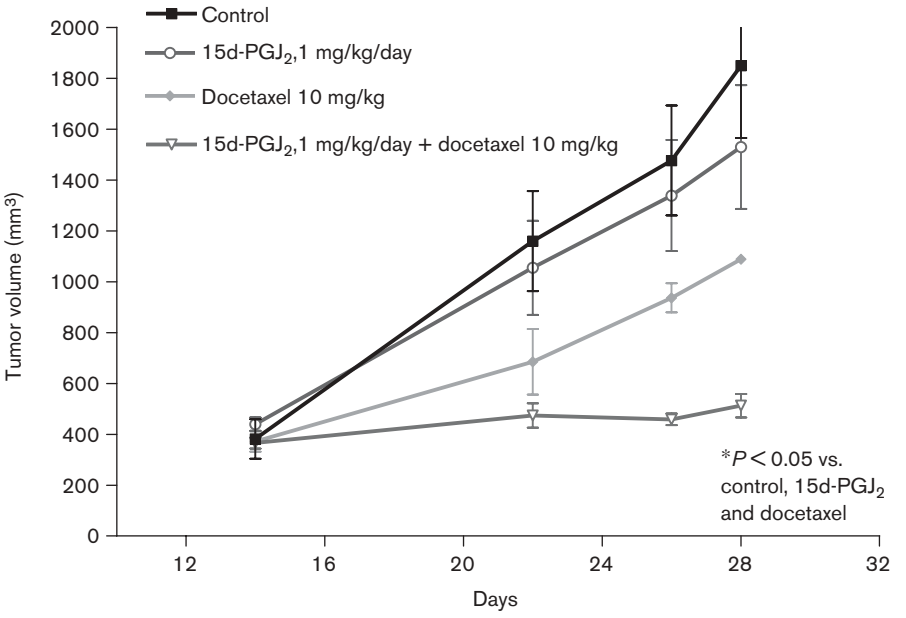

Anti-tumor activity of 15-deoxy-$\Delta^{12,14}$-prostaglandin J$_2$ (15d-PGJ$_2$), docetaxel and 15d-PGJ$_2$ + docetaxel against A549 lung tumors. Treatment with docetaxel and 15d-PGJ$_2$ was initiated 14 days after tumor implantation. Data presented are mean ± SEM. The tumor volume observed in the docetaxel + 15d-PGJ$_2$-treated group was significantly lower with $P < 0.05$ vs. untreated control, 15d-PGJ$_2$ alone and docetaxel alone at days 26 and 28 as analyzed by the non-parametric Mann–Whitney test.

1088.00 ± 80.8 and 512.50 ± 46.0 mm^3 (expressed as mean ± SEM) in vehicle control, 15d-PGJ$_2$, docetaxel and 15d-PGJ$_2$ + docetaxel-treated mice, respectively. These results indicate that there was 72 and 41% reduction in the tumor volume with 15d-PGJ$_2$ + docetaxel and docetaxel-treated mice, respectively. The inhibition was only 17% by 15d-PGJ$_2$ treatment alone. With H460 tumors (Fig. 2), at the end of 28 days, the tumor volumes were found to be 6105 ± 143, 5529 ± 376.6, 2617 ± 168.5 and 1785 ± 111.3 mm^3 (expressed as mean ± SEM) in vehicle control, 15d-PGJ$_2$, docetaxel and 15d-PGJ$_2$ + docetaxel-treated mice, respectively. The inhibition of tumor volume was 70.8 and 57% by 15d-PGJ$_2$ + docetaxel and docetaxel treatment, respectively. Treatment with 15d-PGJ$_2$ reduced the H460 tumors by 9.4%. 15d-PGJ$_2$ + docetaxel showed significant tumor growth inhibition as compared with docetaxel alone in both A549 ($P < 0.05$) and H460 ($P < 0.01$) tumors.

Induction of apoptosis in A549 cells and tumor tissues by docetaxel and the combination of 15-deoxy-$\Delta^{12,14}$-prostaglandin J$_2$ + docetaxel

Figure 3 shows A549 cells undergoing apoptosis following treatment with 0.01 μmol/l docetaxel, 10 μmol/l 15d-PGJ$_2$

Fig. 2

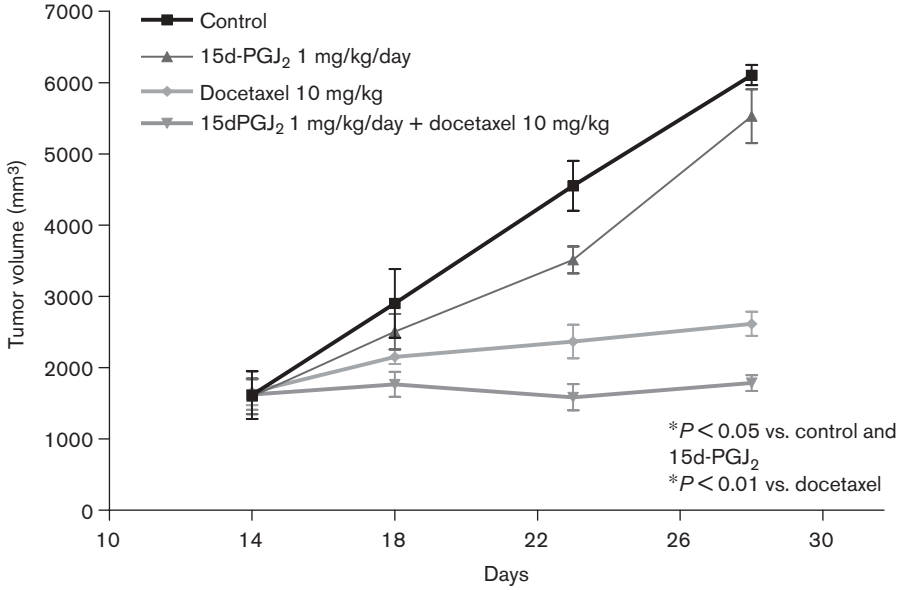

Anti-tumor activity of 15-deoxy-$\Delta^{12,14}$-prostaglandin J_2 (15d-PGJ_2), docetaxel and 15d-PGJ_2 + docetaxel against H460 lung tumors. Treatment with docetaxel and 15d-PGJ_2 was initiated 14 days after tumor implantation. Data presented are mean ± SEM. The tumor volume observed in the docetaxel + 15d-PGJ_2-treated group was significantly lower with $P < 0.05$ vs. untreated control and 15d-PGJ_2 alone; $P < 0.01$ vs. docetaxel alone at day 28 as analyzed by the non-parametric Mann–Whitney test.

and the combination of 0.01 μmol/l docetaxel + 10 μmol/l 15d-PGJ_2. Significant positive TUNEL staining (Fig. 3A, e–h) was observed in A549 cells at 48 h after treatment with 15d-PGJ_2 + docetaxel. Compared with docetaxel alone, 15d-PGJ_2 + docetaxel induced 1.5-fold increase in apoptosis. Although all the treatments showed a significant ($P < 0.001$) increase in apoptosis as compared with control, no positive TUNEL staining was observed in control (untreated) cells. 4,6-Diamidino-2-phenylindole nuclear staining (Fig. 3A, a–d) was used for identification of chromatin condensation, which is an important morphological characteristic of apoptosis. The cells that showed nuclear condensation also demonstrated positive TUNEL staining. Figure 3(B) shows quantification of apoptotic cells following TUNEL assay. Docetaxel and 15d-PGJ_2 + docetaxel treatments also showed significant apoptotic response (40 and 50% increase, respectively) in A549 xenograft tumors as compared with the control tumors. 15d-PGJ_2 alone did not induce any apoptosis as compared with control (data not shown).

Anti-tumor effect of 15-deoxy-$\Delta^{12,14}$-prostaglandin J_2 + docetaxel is associated with reduced intratumor prostaglandin E_{22} levels

Figure 4 shows significant reduction in PGE_2 levels in A549 tumors treated with 15d-PGJ_2 ($P < 0.01$), docetaxel ($P < 0.01$) and 15d-PGJ_2 + docetaxel ($P < 0.001$) as compared with vehicle-treated control mice, reducing the intratumor PGE_2 levels by 41, 49 and 76%, respectively. 15d-PGJ_2 + docetaxel treatment also showed significant inhibition compared with 15d-PGJ_2 ($P < 0.05$) and docetaxel ($P < 0.05$) treatments alone.

15-Deoxy-$\Delta^{12,14}$-prostaglandin J_2 treatment is associated with an increase in peroxisome proliferator-activated receptor-γ protein expression and caspase-3 activation

15d-PGJ_2, docetaxel and 15d-PGJ_2 + docetaxel treatments significantly ($P < 0.001$) increased PPAR-γ protein expression compared with control in A549 tumors. The combination treatment of 15d-PGJ_2 + docetaxel did not, however, significantly increase PPAR-γ expression over docetaxel treatment. Western blotting demonstrated that 15d-PGJ_2 + docetaxel treatment resulted in enhanced expression of caspase-3, whereas its expression was undetectable in tumor tissues from control mice and mice treated with 15d-PGJ_2 and docetaxel (Fig. 5).

Upregulation of caspase family of proteins and downregulation of cyclin D1 mRNA expression by 15-deoxy-$\Delta^{12,14}$-prostaglandin J_2 + docetaxel treatment as studied by real-time polymerase chain reaction

Real-time PCR studies with A549 tumors indicated that there was significant ($P < 0.001$) upregulation of caspase-3 and caspase-8 mRNA expression by 15d-PGJ_2 and 15d-PGJ_2 + docetaxel treatment compared with control (Fig. 6). Docetaxel alone also induced significant increase in caspase-3 ($P < 0.001$) and -8 ($P < 0.01$) as compared

Fig. 3

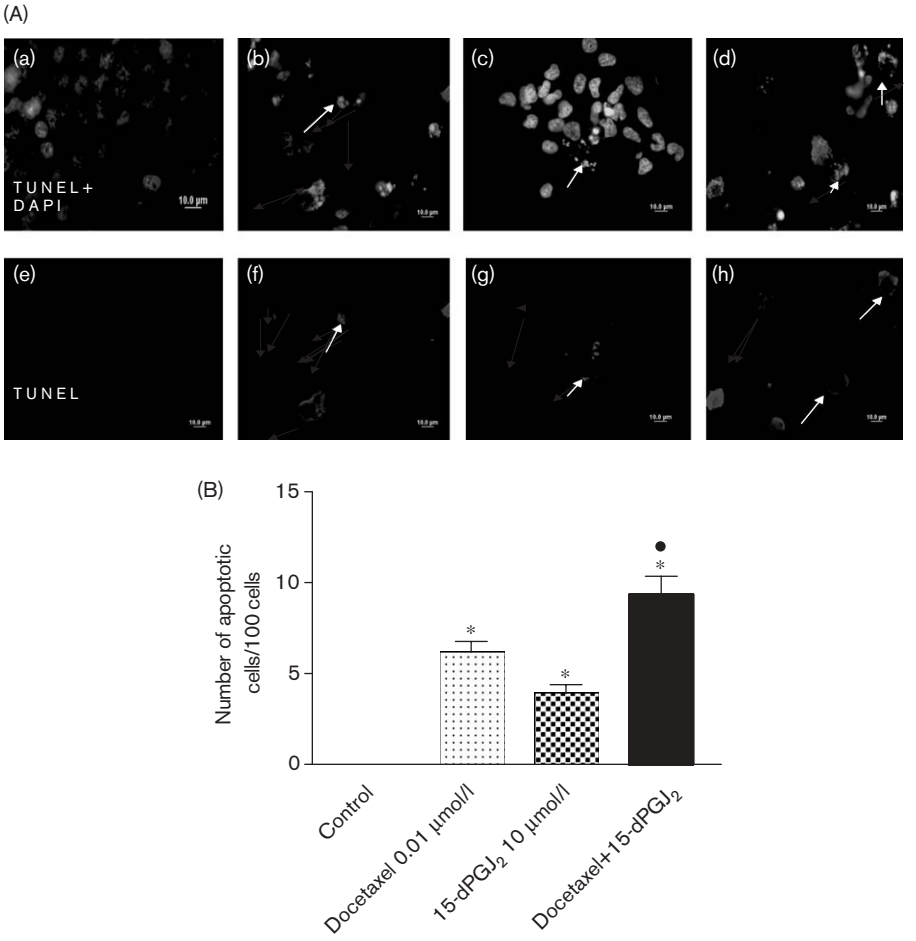

(A) Fluorescence micrographs of differentiated A549 cells stained with terminal deoxynucleotidyl transferase-mediated deoxyuridine triphosphate-biotin nick-end-labeling (TUNEL) and 4,6-diamidino-2-phenylindole (DAPI) after 48-h treatment with 0.01 μmol/l docetaxel (b and f), 15dPGJ$_2$ 10 μmol/l (c and g) and the combination of docetaxel 0.01 μmol/l + 15d-PGJ J$_2$ 10 μmol/l (d and h). DNA fragmentation indicated by positive staining (red) (e and h) and nuclear condensation indicated by DAPI nuclear staining (blue). Control (a and e) cells were untreated. Micron bar = 10 μm. (B) Quantification of apoptotic cells from the TUNEL assay; 100 cells from six random microscopic fields were counted. Data are expressed as mean ± SD (n = 6). One-way analysis of variance followed by Tukey multiple comparisons test was used for statistical analysis to compare control and treated groups. *P < 0.001 vs. control, •P < 0.01 vs. docetaxel.

with control. Although caspase-9 expression was significantly ($P < 0.001$) upregulated by docetaxel and 15d-PGJ$_2$ + docetaxel ($P < 0.05$), there was no significant alteration ($P > 0.05$) by 15d-PGJ$_2$. Cyclin D1 mRNA levels were significantly downregulated by 15d-PGJ$_2$, docetaxel and 15d-PGJ$_2$ + docetaxel treatments as compared with control (Fig. 7). 15d-PGJ$_2$ + docetaxel also showed significant ($P < 0.05$) downregulation of cyclin D1 as compared with docetaxel treatment alone.

Alteration of Bcl2 and p53 family protein mRNA expression by 15-deoxy-$\Delta^{12,14}$-prostaglandin J$_2$, docetaxel and 15-deoxy-$\Delta^{12,14}$-prostaglandin J$_2$ + docetaxel treatment as studied by reverse transcription-polymerase chain reaction

In A549 tumor samples, studies with the Bcl2 family of proteins showed that all the three treatments significantly ($P < 0.001$) increased BAD mRNA expression, whereas there was significant ($P < 0.001$) downregulation of Bcl2 mRNA levels (Fig. 8). 15d-PGJ$_2$ + docetaxel showed significantly upregulated BAD ($P < 0.001$) and downregulated Bcl2 ($P < 0.05$) as compared with docetaxel treatment alone. In the p53 family mRNA expression study with the A549 tumor tissues, 15d-PGJ$_2$ + docetaxel treatment significantly ($P < 0.001$) increased apoptotic protease-activating factor (APAF1) ($P < 0.001$), Bcl2-binding component (BBC3) ($P < 0.001$) and tumor-suppressor protein p53 expression ($P < 0.01$) as compared with docetaxel treatment (Fig. 9). By itself, docetaxel treatment also significantly induced expression of all the three p53 family proteins compared with control. Treatment with 15d-PGJ$_2$ significantly ($P < 0.001$) altered the mRNA levels for APAF1 without changing the expressions of BBC3 and p53.

Fig. 4

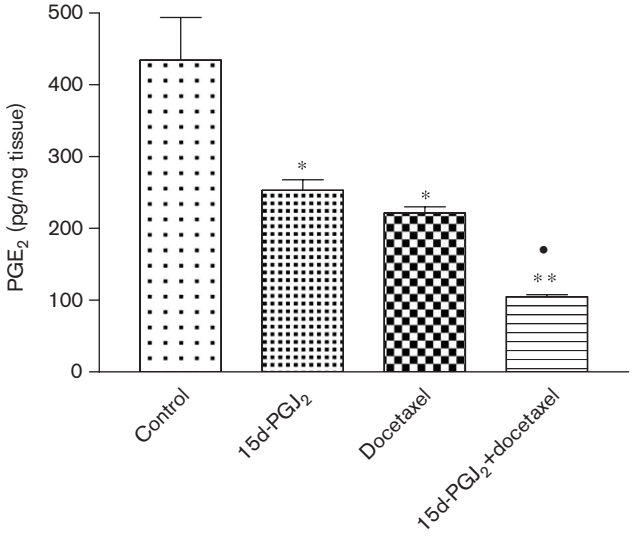

Intratumor prostaglandin E_2 (PGE_2) levels in A549 lung tumors assayed using enzyme immunoassay kits. The treatments significantly lowered the PGE_2 levels compared with control. Data points represent the mean of triplicate determinations from two separate experiments. Error bars depict standard deviations. *$P<0.01$, **$P<0.001$ vs. untreated control, •$P<0.05$ vs. docetaxel.

Fig. 5

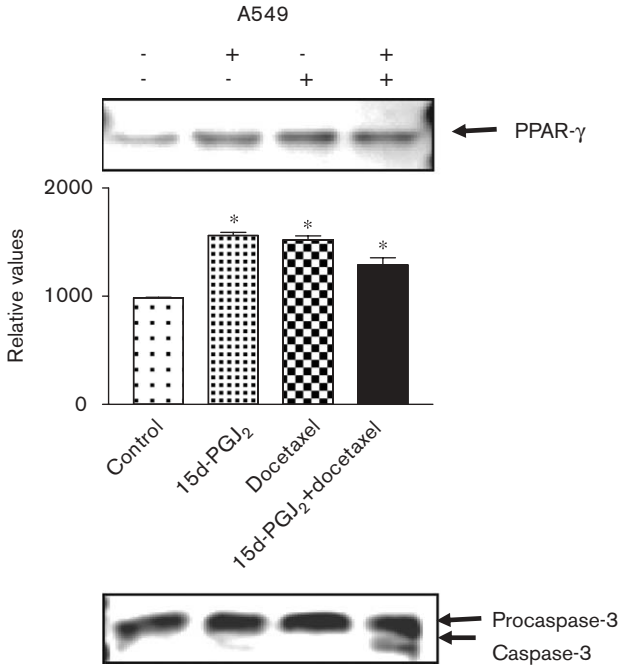

Western blotting of tumor tissue lysates to determine peroxisome proliferator-activated receptor (PPAR-γ) and caspase-3 protein expressions. The tumors were harvested 28 days after tumor implantation and lysates were prepared as described in Materials and methods. Thirty micrograms of protein was loaded in each lane. Data points represent the mean of triplicate determinations from two separate experiments. *$P<0.001$ vs. untreated control.

Fig. 6

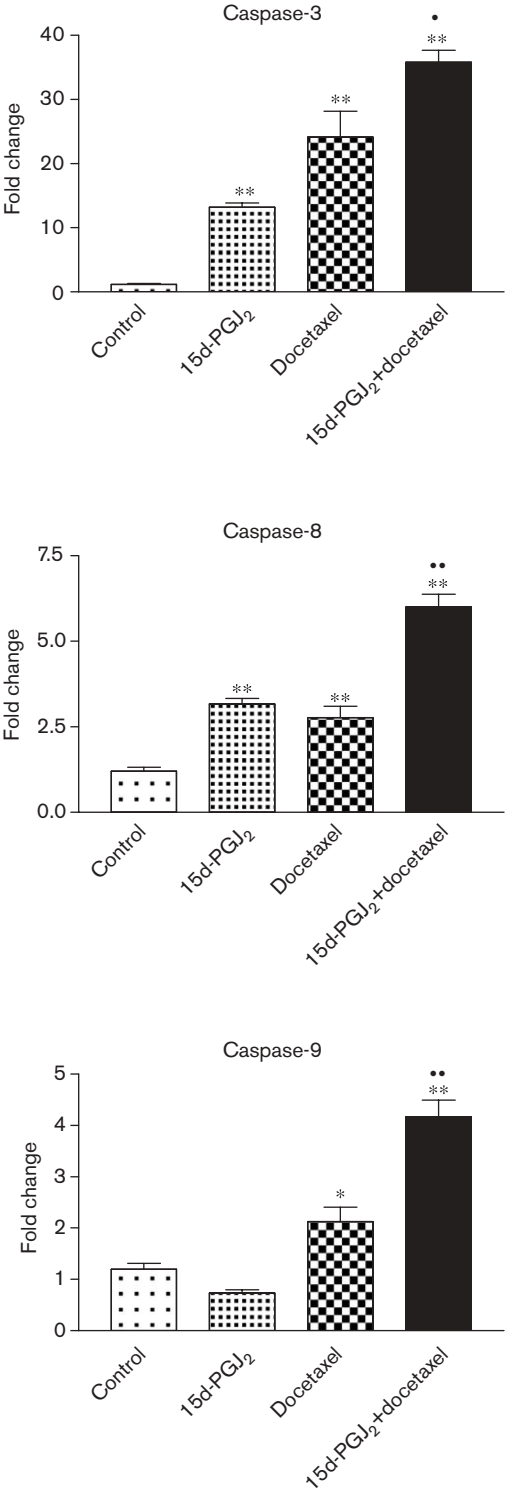

Real-time polymerase chain reaction study to detect the mRNA levels of caspase-3, caspase 8 and caspase-9 in the tumor tissues after 15d-PGJ_2, docetaxel and 15d-PGJ_2 + docetaxel treatments compared to untreated control. Data points represent the mean of quadruplicate determinations from two separate experiments. Error bars depict standard deviations. *$P<0.05$, **$P<0.01$ vs. untreated control; •$P<0.01$ and ••$P<0.001$ vs. docetaxel.

Fig. 7

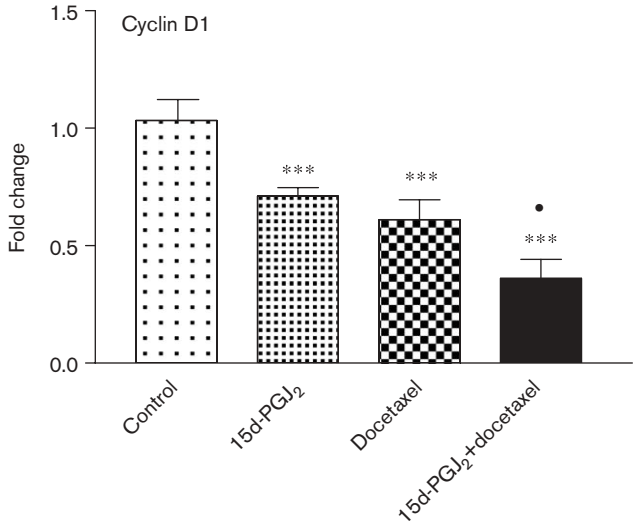

Real-time polymerase chain reaction study to detect the mRNA levels of cyclin D1 in the A549 tumor tissues after 15d-PGJ$_2$ docetaxel and $_2$ + 15d-PGJ$_2$ docetaxel treatments compared to untreated control. Data points represent the mean of quadruplicate determinations from two separate experiments. Error bars depict standard deviations $^{**}P<0.01$ vs. untreated control, $^{\bullet}P<0.05$ vs. docetaxel.

Peroxisome proliferator-activated receptor-γ independent caspase-3 and cyclin D1 expression in A549 cell line

A549 cells treated with 15d-PGJ$_2$ and 15d-PGJ$_2$ + docetaxel showed a significant ($P < 0.001$) increase in PPAR-γ expression as compared with control, which was significantly ($P < 0.001$) reduced by treatment with GW9662, a potent PPAR-γ antagonist (Fig. 10). Docetaxel did not show any increase in PPAR-γ expression in A549 cells in the presence or absence of GW9662. Further, all the treatments except GW9662 significantly ($P < 0.001$) increased caspase-3 expression compared with untreated control in the A549 cell line. Treatment with GW9662 did not significantly alter the 15d-PGJ$_2$, docetaxel and 15d-PGJ$_2$ + docetaxel-induced increase in caspase-3 expression. Significant downregulation of cyclin D1 mRNA levels was observed with A549 tumor cells treated with 15d-PGJ$_2$, docetaxel and 15d-PGJ$_2$ + docetaxel as compared with control that did not alter even by pretreatment of A549 cells with GW9662 as shown in Fig. 10.

Discussion

PPAR-γ has been studied over the past decade for its important role in the regulation of cellular metabolism. It functions as an important regulator of lipid and glucose metabolism, adipocyte differentiation, and energy homeostasis [18]. Activation of PPAR-γ resulted in decreased concentration of serum glucose in diabetes, which led to the development of PPAR-γ agonists that are now in clinical use as anti-diabetic drugs (e.g. pioglitazone and rosiglitazone).

Fig. 8

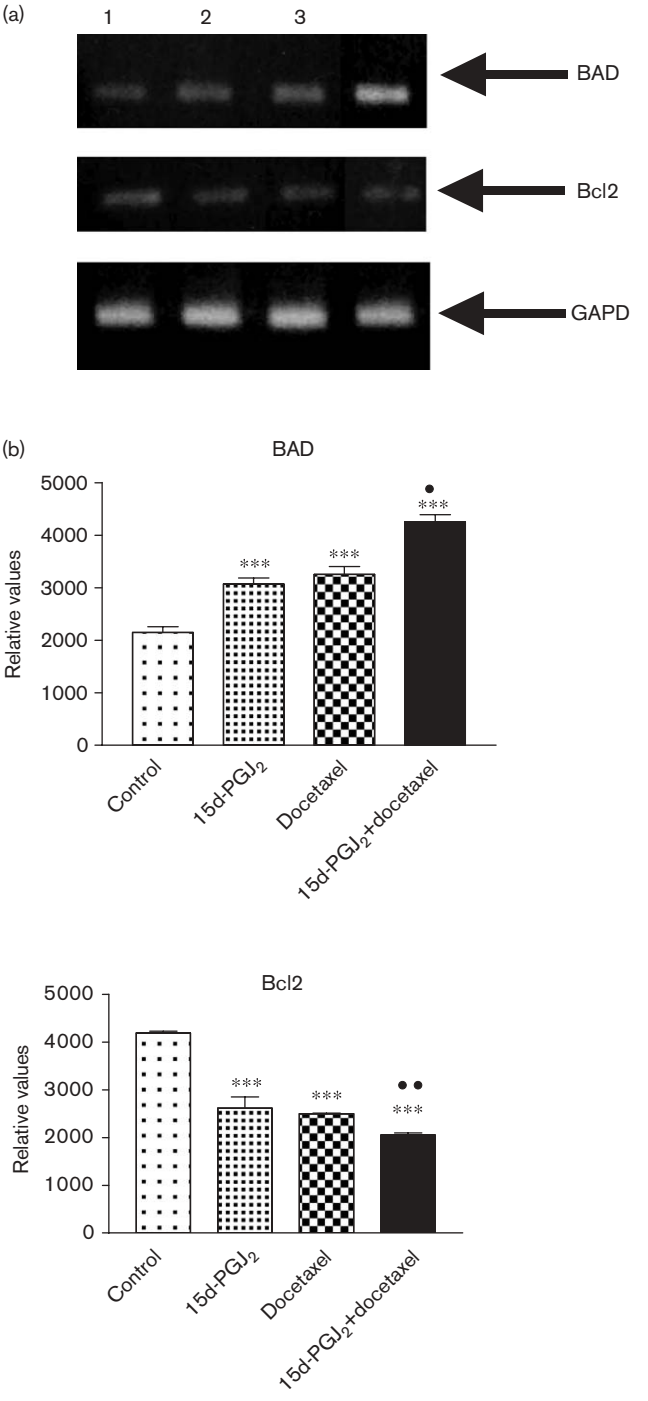

Expression of BAD, Bcl2 and GAPD mRNA in xenograft human A549 lung tumors by reverse transcription-polymerase chain reaction (RT-PCR). RNAs were isolated from the tumor tissues, reverse transcribed using random hexamers and amplified by PCR as described in detail under Materials and methods. (a) The RT-PCR products were electrophoresed on ethidium bromide-containing 2% agarose gels. (b) The densitometric analysis of the bands was performed using the program ImageJ v1.33u. Error bars depict standard deviations. $^{***}P<0.001$ vs. untreated control; $^{\bullet}P<0.001$ and $^{\bullet\bullet}P<0.05$ vs. docetaxel.

Fig. 9

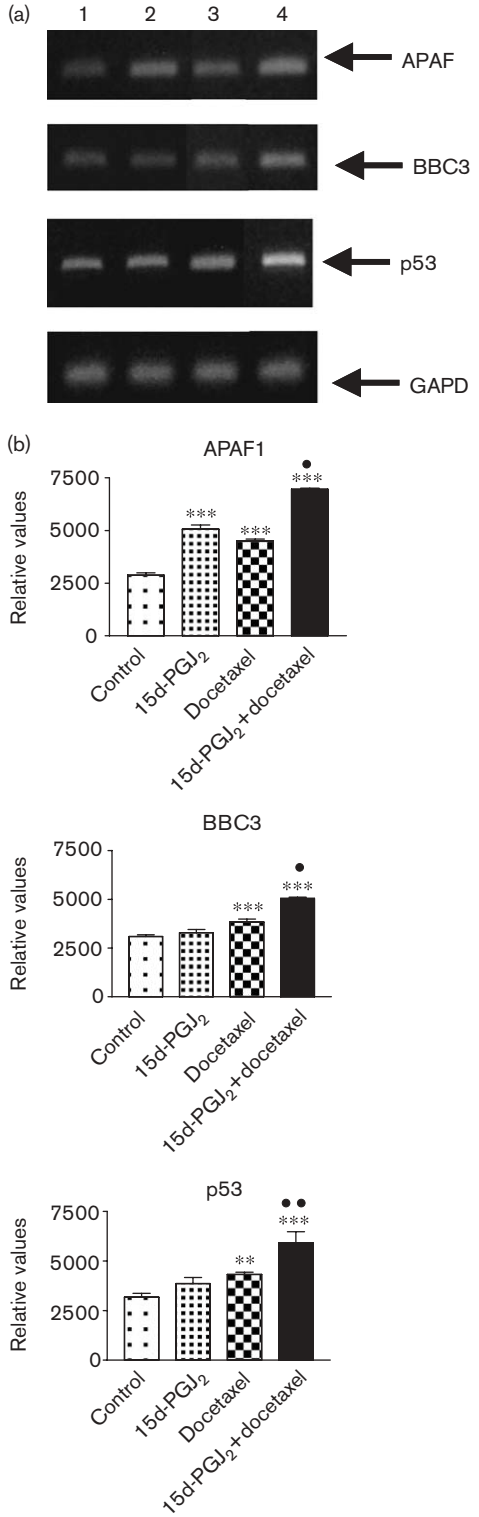

Expression of apoptotic protease-activating factor (APAF) 1, BBC3, p53 (p53 family members) and GAPD mRNA in xenograft human A549 lung tumors by reverse transcription-polymerase chain reaction (RT-PCR). RNAs were isolated from the tumor tissues, reverse transcribed using random hexamers and amplified by PCR as described in detail under Materials and methods. (a) The RT-PCR products were electrophoresed on ethidium bromide-containing 2% agarose gels. (b) The densitometric analysis of the bands was performed using the program ImageJ v1.33u. Error bars depict standard deviations. $^{**}P<0.01$ and $^{***}P<0.001$ vs. untreated control; $^{\bullet}P<0.001$ and $^{\bullet\bullet}P<0.01$ vs. docetaxel.

Fig. 10

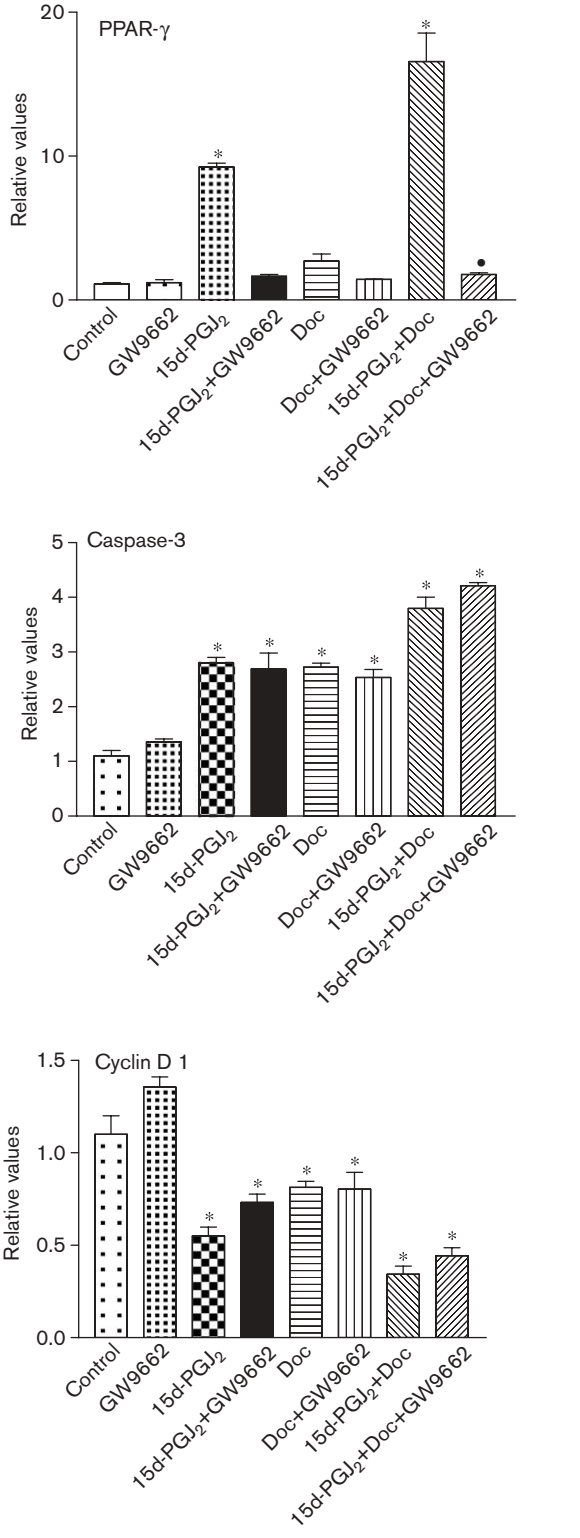

Real-time polymerase chain reaction study to detect the mRNA levels of peroxisome proliferator-activated receptor (PPAR-γ), caspase-3 and cyclin D1 in the A549 cells after 15-deoxy-$\Delta^{12,14}$-prostaglandin J_2 (15d-PGJ_2), docetaxel and 15d-PGJ_2 + docetaxel treatments compared with untreated control in the presence and absence of GW9662. Data points represent the mean of quadruplicate determinations from two separate experiments. Error bars depict standard deviations. $^{*}P<0.001$ vs. untreated control, $^{\bullet}P<0.001$ vs. 15d-PGJ_2 + docetaxel.

Apart from established metabolic actions, PPAR-γ agonists have been found to induce apoptosis in several malignant cell lines like breast, pancreas, colon and NSCLC [15,19–21]. These findings initiated further research to assess the potential of PPAR-γ agonists as a promising new therapeutic alternative in the treatment of cancer.

In the present study, isobolographic analysis demonstrated that 15d-PGJ$_2$ potentiates the cytotoxicity of docetaxel in human lung cancer cells (A549 and H460) and the nature of the interaction is synergistic. As shown in Table 1, the CI values against both the cell lines at different concentrations of 15d-PGJ$_2$ were less than 1.0, indicative of synergistic interaction. We previously showed that celecoxib exhibits similar dose-dependent enhancement of docetaxel activity against lung cancer cell lines [6]. Our data are in agreement with the work of Menendez *et al.* [22] who demonstrated by isobolographic analysis the ability of exogenous fatty acids to modulate the cytotoxic activity of anti-cancer drugs like doxorubicin in breast cancer cell lines. The CI values ranged from 0.799 to 1.170 for 5–95% cell kill levels, suggesting slight to moderate synergism or nearly additive interactions [22]. Similarly, Kim *et al.* [23] showed that simultaneous exposure to troxacitabine and camptothecin shows a synergistic effect in oropharyngeal KB cells (CI = 0.2–0.8) but only additive in HepG2 cells (CI = 1.0), demonstrating that the effect was not only dose dependent but also cell line specific. Also, Talcott and Percival [24] demonstrated the apparent synergistic interaction for the combinations of ellagic acid with resveratrol (CI = 0.64) and quercetin with resveratrol (CI = 0.68) in the induction of caspase-3 activity. Their results indicated that the anti-carcinogenic potential of foods containing polyphenols may not be based on the effects of individual compounds, but may involve a synergistic enhancement of the anti-cancer effects [24].

This is the first in-vivo study with 15d-PGJ$_2$ in mice xenografted with A549 and H460 lung tumors; therefore, we focused on the anti-tumor mechanism of 15d-PGJ$_2$ by itself and in combination with docetaxel. Although 15d-PGJ$_2$ potentiated docetaxel anti-tumor activity against both A549 and H460 cell lines, detailed mechanistic studies were conducted only against A549 cells and xenograft tumors as the data obtained from H460 cells was equally comparable. In the current study, we followed the work of Cuzzocrea *et al.* [25] for our in-vivo treatment dose selection [25]. Cuzzocrea *et al.* investigated the effects of 15d-PGJ$_2$ in acute and chronic inflammation (carrageenan-induced pleurisy and collagen-induced arthritis, respectively) in BALB/c and DBA/1J mice. They reported that 15d-PGJ$_2$ (given at 10, 30 or 100 μg/kg intraperitoneally in the pleurisy model or 30 μg/kg intraperitoneally every 48 h in the arthritis model) exerted potential anti-inflammatory effect. Our study being in a xenografted tumor model in which we started 15d-PGJ$_2$ treatment 14 days after tumor induction, we selected a higher dose of 1 mg/kg/day. For docetaxel administration (10 mg/kg; 3 times), we followed a modified protocol on the basis of the studies by Dykes *et al.* [26] in which they used a higher effective dose (22 mg/kg, 3 times) in LX-1 lung tumor xenografts. For the combination of 15d-PGJ$_2$ with docetaxel, 15d-PGJ$_2$ treatment was initiated at day 14 following tumor implantation when the first docetaxel dose was administered. Our rationale for selecting a delayed treatment protocol was to study the treatment efficacy in advanced lung tumors more simulating the real patient scenario. It is evident from Fig. 1 that in the A549 tumor model, the combination of 15d-PGJ$_2$ with docetaxel resulted in higher inhibition of tumor growth than the control, 15d-PGJ$_2$ and docetaxel treatments. Further, in an aggressive H460 tumor model, the combination of 15d-PGJ$_2$ + docetaxel showed a more pronounced and significant ($P < 0.05$) growth inhibition as compared with all other treatments. The enhancement of anti-tumor effect of docetaxel by 15d-PGJ$_2$ is promising, because the treatments (15d-PGJ$_2$, docetaxel and 15d-PGJ$_2$ + docetaxel) were initiated at day 14 after tumor implantation when the average tumor volumes were 300 and 1500 mm^3 in A549 and H460 tumors, respectively [6].

We measured the intratumor PGE$_2$ levels and found significant reduction in PGE$_2$ levels in A549 tumors obtained from mice treated with 15d-PGJ$_2$ ($P < 0.01$), docetaxel ($P < 0.01$) and 15d-PGJ$_2$ + docetaxel ($P < 0.001$) as compared with vehicle-treated control mice. With 15d-PGJ$_2$ + docetaxel treatment, there was a significant ($P < 0.05$) decrease in PGE$_2$ levels as compared with docetaxel treatment. Further, we observed an increase in PPAR-γ protein levels following treatments with 15d-PGJ$_2$, docetaxel and 15d-PGJ$_2$ + docetaxel in A549 tumors (Fig. 5). The increase in PPAR-γ protein expression by docetaxel did not correlate with the in-vitro findings (Fig. 10), which may be attributed to the difference in dose and treatment schedules adopted *in vitro* and *in vivo*. PPAR-γ activation suggests inhibition of the COX-2 pathway, which leads to the inhibition of prostaglandin synthesis. Our results are in agreement with earlier findings by Li *et al.* [27] in which they found that PPAR-γ activation resulted in apoptosis and COX-2 inhibition in liver cancer (HepG2) cells. Other researchers have, however, also suggested the existence of PPAR-γ-independent anti-tumor activity for 15d-PGJ$_2$ [28–31].

PPAR-γ agonists show anti-neoplastic effects by inducing apoptosis [32]. Earlier in-vitro studies with troglitazone and 15d-PGJ$_2$ in lung cancer cell lines (H841, A549, PC14) showed that they inhibited cell growth and induced apoptosis [33]. In the present study, we report that PPAR-γ natural ligand 15d-PGJ$_2$ enhanced anti-tumor activity of docetaxel and induced apoptosis. This is in agreement with other investigations by different

groups demonstrating the involvement of 15d-PGJ_2 in apoptosis-related cell growth inhibition or cell cycle arrest induced by 15d-PGJ_2 [10,18,34–36]. Studies with novel synthetic PPAR-γ activators like 1,1-bis (3'indolyl)-1-(*p*-substituted phenyl) methanes containing *p*-trifluoromethyl (DIM-C-pPhCF_3), *p*-*t*-butyl (DIM-C-pPhtBu) and *p*-phenyl (DIM-C-pPhC_6H_5) in colon cancer cells HT-29, HCT-15 and breast cancer cell line MCF-7 also showed growth inhibition and cell cycle arrest at G_0/G_1–S phase [37,38]. Docetaxel and 15d-PGJ_2 + docetaxel showed significant apoptotic response in A549 cells (Fig. 3) and almost 40–50% increase in apoptosis in A549 tumors, respectively, as compared with the control (data not shown). Caspases prove to be one of the key mechanisms in the induction of apoptosis. Studies with malignant astrocytes and human liver cancer showed that PPAR-γ activation leads to increase in caspase-3 activity [39,40]. Shimada *et al.* reported that troglitazone treatment in colon cancer cells induced cell death and apoptosis, which was prevented by pan-caspase inhibitors. We observed significant increase in caspase-3, -8 and -9 as a result of docetaxel and 15d-PGJ_2 + docetaxel treatments (Fig. 6). Although 15d-PGJ_2 by itself did increase caspase-3 and -8, there was no significant increase in caspase-9 compared with control in A549 tumors (Fig. 6). It is known that procaspase-8 leads to caspase-8 formation, which can trigger caspase-3 release leading to apoptosis. The increase in the caspases-3 and -8 by 15d-PGJ_2 treatment, although significantly higher than control, may not have reached the threshold where it could significantly induce apoptosis. Caspase-9, on the other hand, is activated from procaspase-9 by upregulation of APAF1, which forms a complex with cytochrome *c*. This active caspase-9 can also directly trigger caspase-3 release and apoptosis. Both the caspase-9 mRNA level (Fig. 6) and the results of apoptosis study after 15d-PGJ_2 treatment showed a correlation indicating no change compared with control.

We hypothesized that the induction of apoptosis in 15d-PGJ_2 + docetaxel-treated A549 lung tumors is not only mediated by caspases, but also there is involvement of Bcl2 and p53 family (APAF1) pathways. Zander *et al.* [41] studied C6 glioma cells and found that upregulation of pro-apoptotic BAX and BAD had a functional role in apoptotic cell death. BAD and BAX upregulated expression released cytochrome *c* and subsequent activation of several effector caspases. Hence, we investigated the levels of pro-apoptotic BAD and anti-apoptotic Bcl2 in A549 lung tumors as a result of 15d-PGJ_2, docetaxel and 15d-PGJ_2 + docetaxel treatments. We found that our treatments increased BAD mRNA levels and decreased Bcl2 (Fig. 8). Overexpression of Bcl2 is correlated with the progression of malignancy. A recent report suggested that ectopic expression of Bcl2 could impair apoptotic signaling by inactivating c-Jun NH_2-terminal kinase, leading to inhibition of apoptosis [42]. BAD, on the other hand, is a pro-apoptotic BH3-only member of Bcl2 family. The increase in BAD and decrease in Bcl2 triggers the mitochondrial cytochrome *c* release [41].

APAF1 is the structural core of the apoptosome. When the mitochondrial pathway of apoptosis is activated, cytochrome *c* is released from mitochondria to cytosol and then binds to APAF1 CARD domain changing its conformation. A further binding of ATP molecules mediates a second conformational change, which leads to the open APAF1 conformation. By means of the CARD domain, seven APAF1 molecules bind to each other and to seven molecules of initiator caspase-9, forming the apoptosome and causing the activation of effector caspases. The formation of the apoptosome and the activation of caspases are regulated by numerous interacting proteins [43]. To get a better understanding of this mechanism, in our current investigation, we looked at the levels of p53 family proteins. We observed that the combination of 15d-PGJ_2 + docetaxel produced a significant increase in the expression of APAF1, BBC3 and p53 proteins in A549 tumors (Fig. 9). Therefore, we believe that the combined treatment of 15d-PGJ_2 + docetaxel triggered Bcl2 pathway, p53-related APAF1 upregulation, which triggered the formation of caspase-9 followed by caspase-3 leading to apoptosis.

PPAR-γ agonists also have been studied in relation to their anti-proliferative effects. PPAR-γ agonists promote cell cycle arrest by the downregulation of cyclin D1 in several tumor cell lines, including those derived from pancreatic cancer [44], breast cancer [45], hepatocellular carcinoma [46] and NSCLC [21]. PPAR-γ downregulates cyclin D1 by transcriptional repression involving competition between PPAR-γ and c-fos for a limited supply of coactivator p300 [47]. Consistent with these results, we observed that 15d-PGJ_2, docetaxel and 15d-PGJ_2 + docetaxel treatments inhibited cyclin D1 levels in A549 lung tumors (Fig. 7).

Having studied the pathways leading to apoptosis after 15d-PGJ_2, docetaxel and 15d-PGJ_2 + docetaxel treatments, we wanted to investigate the involvement of PPAR-γ-independent mechanisms. Recent studies have suggested that although PPAR-γ is involved in differentiation and cellular metabolic changes after ligand binding, PPAR-γ-independent effects have also been proposed for PPAR-γ agonists. 15d-PGJ_2 inhibits the secretion of tumor necrosis factor-α and interleukin-6 in macrophages stimulated by bacterial lipopolysaccharide and directly blocks IκB kinase complexes in a PPAR-γ-independent way through inhibition of IκB kinases [48]. Further, sensitivity of cancer cell lines to glitazone-induced growth inhibition does not correlate with amounts of PPAR-γ protein. Thus, glitazone resistance occurs in tumors even with high PPAR-γ levels, e.g.

breast tumor cells [34]. In the present study, we used a PPAR-γ inhibitor GW9662 to inhibit the PPAR-γ activity, and observed that there was no change in the mRNA levels of caspase-3 and cyclin D1, the key molecules in apoptosis and cell cycle regulation (Fig. 10). This suggests involvement of a PPAR-γ-independent pathway in the anti-tumor effects observed. Qin *et al.* [38] studied the PPAR-γ-independent mechanisms of C-substituted DIMs and PGJ$_2$ in MCF-7 cells. They demonstrated that PPAR-γ inhibitor T007 did not affect the downregulation of cyclin D1 or ERα by PGJ2 or DIM-C-pPhCF$_3$, indicating that their anti-tumor response was PPAR-γ-independent. In another study, 2-cyabo-3,12-diooxoolean-1,9-dien-oic acid and related PPAR-γ agonists have been shown to induce caveolin-1 in colon cancer cells and this effect was inhibited by PPAR-γ antagonists, whereas higher concentrations of 2-cyabo-3,12-diooxoolean-1, 9-dien-oic acid induced apoptosis in PPAR-γ-independent fashion even in the presence of PPAR-γ antagonists [49]. On similar lines, in the present study we observed that GW9662 did not alter the 15d-PGJ$_2$, docetaxel and 15d-PGJ$_2$ + docetaxel upregulated caspase 3 and downregulated cyclin D1 levels in A549 cells. These studies thus suggest a possible role of PPAR-γ-independent pathway for the anti-tumor effect induced by 15d-PGJ$_2$ + docetaxel, which has also been demonstrated by other workers. Currently, studies are in progress in our laboratory to investigate these mechanisms in greater detail. Considering the fact that 15d-PGJ$_2$ + docetaxel downregulated cyclin D1, efforts are also being made to understand the effect of the combination on cell cycle arrest in NSCLC cell lines.

In conclusion, we have demonstrated for the first time in an in-vivo animal model that a PPAR-γ natural ligand 15d-PGJ$_2$ significantly potentiated the activity of docetaxel and the combination caused tumor regression, induced apoptosis and cell cycle arrest in A549 and H460 human lung tumors by PPAR-γ-dependent and PPAR-γ-independent pathways. The combined treatment of 15d-PGJ$_2$ + docetaxel showed significantly superior treatment efficacy than 15d-PGJ$_2$ and docetaxel treatments alone. Hence, this study validates the use of 15d-PGJ$_2$ in combination with anti-cancer agents as potential new therapeutic approach in the treatment of lung cancer.

Acknowledgements

We are thankful to Aventis (Collegeville, Pennsylvania, USA) for the gift sample of docetaxel.

References

1 Mathieu A, Remmelink M, D'Haene N, Penant S, Gaussin JF, Van Ginkel R, *et al.* Development of a chemoresistant orthotopic human non-small cell lung carcinoma model in nude mice: analyses of tumor heterogeneity in relation to the immunohistochemical levels of expression of cyclooxygenase-2, ornithine decarboxylase, lung-related resistance protein, prostaglandin E synthetase, and glutathione-*S*-transferase-alpha (GST)-alpha, GST-mu, and GST-pi. *Cancer* 2004; **101**:1908–1918.

2 Nguyen TT, Tran E, Nguyen TH, Do PT, Huynh TH, Huynh H. The role of activated MEK–ERK pathway in quercetin-induced growth inhibition and apoptosis in A549 lung cancer cells. *Carcinogenesis* 2004; **25**:647–659.

3 Gargiullo P, Wingo PA, Coates RJ, Thompson TD. Recent trends in mortality rates for four major cancers, by sex and race/ethnicity – United States. *Morb Mortal Weekly Rep* 2002; **51**:49–53.

4 Hida T, Leyton J, Makheja AN, Ben Av P, Hla T, Martinez A, *et al.* Non-small cell lung cancer cyclooxygenase activity and proliferation are inhibited by non-steroidal antiinflammatory drugs. *Anticancer Res* 1998; **18**:775–782.

5 Hida T, Kozaki KI, Muramatsu H, Bev AvP, Hla T, Martinez A, *et al.* Cyclooxygenase-2 inhibitor induces apoptosis and enhances cytotoxicity of various anticancer agents in non-small cell lung cancer cell lines. *Clin Cancer Res* 2000; **6**:2006–2011.

6 Shaik MS, Chatterjee A, Jackson T, Singh M. Enhancement of antitumor activity of docetaxel by celecoxib in lung tumors. *Int J Cancer* 2006; **118**:396–404.

7 Haynes A, Shaik MS, Chatterjee A, Singh M. Formulation and evaluation of aerosolized celecoxib for the treatment of lung cancer. *Pharm Res* 2005; **22**:427–439.

8 Solomon SD, McMurray JJ, Pfeffer MA, Wittes J, Fowler R, Finn P, *et al.* Cardiovascular risk associated with celecoxib in a clinical trial for colorectal adenoma prevention. *N Engl J Med* 2005; **352**:1071–1080.

9 Badawi AF, Eldeen M, Liu Y, Ross EA, Badr MZ. Inhibition of rat mammary gland carcinogenesis by simultaneous targeting of cyclooxygenase-2 and peroxisome proliferator-activated receptor γ. *Cancer Res* 2004; **64**:1181–1189.

10 Nikitakis NG, Hebert C, Lopes MA, Reynolds MA, Sauk JJ. PPAR gamma-mediated antineoplastic effect of NSAID sulindac on human oral squamous carcinoma cells. *Int J Cancer* 2002; **98**:817–823.

11 Wick M, Hurteau G, Dessev C, Chan D, Geraci MW, Winn RA, *et al.* Peroxisome proliferator-activated receptor-γ is a target of nonsteroidal in-inflammatory drugs mediating cyclooxygenase-independent inhibition of lung cancer cell growth. *Mol Pharmacol* 2002; **62**: 1207–1214.

12 Shaik MS, Chatterjee A, Singh M. Effect of a selective cyclooxygenase (COX)-2 inhibitor, nimesulide on the growth of lung tumors and their expression of COX-2 and peroxisome proliferator-activated receptor-γ. *Clin Cancer Res* 2004; **10**:1521–1529.

13 Mueller E, Smith M, Sarraf P, Kroll T, Aiyer A, Kaufamn DS, *et al.* Effects of ligand activation of peroxisome proliferator-activated receptor gamma in human prostate cancer. *Proc Natl Acad Sci U S A* 2000; **97**:10990–10995.

14 Grau R, Iniguez MA, Fresno M. Inhibition of activator protein 1 activation, vascular endothelial growth factor, and cyclooxygenase-2 expression by 15-deoxy-delta12,14-prostaglandin J$_2$ in colon carcinoma cells: evidence for a redox-sensitive peroxisome proliferator-activated receptor-gamma-independent mechanism. *Cancer Res* 2004; **64**:5162–5171.

15 Elstner E, Muller C, Koshizuka K, Williamson EA, Park D, Asou H, *et al.* Ligands for peroxisome proliferator-activated receptorgamma and retinoic acid receptor inhibit growth and induce apoptosis of human breast cancer cells *in vitro* and in BNX mice. *Proc Natl Acad Sci U S A* 1998; **95**:8806–8811.

16 Forman BM, Tontonoz P, Chen J, Brun RP, Spiegelman BM, Evans RM. 15-Deoxy-delta12,14-prostaglandin J$_2$ is a ligand for the adipocyte determination factor PPAR gamma. *Cell* 1995; **83**:803–812.

17 Kliewer SA, Lenhard JM, Willson TM, Patel I, Morris DC, Lehmann JM. A prostaglandin J$_2$ metabolite binds peroxisome proliferator-activated receptor gamma and promotes adipocyte differentiation. *Cell* 1995; **83**:813–819.

18 Chinetti G, Griglio S, Antonucci M, Torra IP, Deleviere P, Majd A, *et al.* Activation of proliferator-activated receptors α and γ induces apoptosis of human monocyte-derived macrophages. *J Biol Chem* 1998; **273**:25573–25580.

19 Eibl G, Wente MN, Reber HA, Hines OJ. Peroxisome proliferator-activated receptor gamma induces pancreatic cancer cell apoptosis. *Biochem Biophys Res Commun* 2001; **287**:522–529.

20 Yang WL, Frucht H. Activation of the PPAR pathway induces apoptosis and COX-2 inhibition in HT-29 human colon cancer cells. *Carcinogenesis* 2001; **9**:1379–1383.

21 Chang TH, Szabo E. Induction of differentiation and apoptosis by ligands of peroxisome proliferator-activated receptor gamma in non-small cell lung cancer. *Cancer Res* 2000; **60**:1129–1138.

22 Menendez J, Barbacid M, Montero S, Sevilla E, Escrich E, Solanas M, *et al.* Effects of gamma-linoleic acid and oleic acid on paclitaxel cytotoxicity in human breast cancer cells. *Eur J Cancer* 2001; **37**:402–413.

23 Kim TE, Park SY, Hsu CH, Dutschman GE, Cheng YC. Synergistic antitumor activity of Troxacitabine and Camptothecin in selected human cancer cell lines. *Mol Pharmacol* 2004; **66**:285–292.

24 Talcott SU, Percival SS. Ellagic acid and quercetin interact synergistically with resveratrol in the induction of apoptosis and cause transient cell cycle arrest in human leukemia cells. *Cancer Lett* 2005; **218**:141–151.

25 Cuzzocrea S, Wayman NS, Mazzon E, Dugo L, Di Paola R, Serriano I, *et al.* The cyclopentenone prostaglandin 15-deoxy Δ12,14-prostaglandin J_2 attenuates the development of acute and chronic inflammation. *Mol Pharmacol* 2002; **61**:997–1007.

26 Dykes DJ, Bissery MC, Harrison SD Jr, Waud WR. Response of human tumor xenografts in athymic nude mice to docetaxel (RP56976, taxotere). *Invest New Drugs* 1995; **13**:1–11.

27 Li MY, Deng H, Zhao JM, Dai D, Tan XY. PPARgamma pathway activation results in apoptosis and COX-2 inhibition in HepG2 cells. *World J Gastroenterol* 2003; **9**:1220–1226.

28 Mueller E, Sarraf P, Tontonoz P, Evan RM, Martin JZ, Zhang M, *et al.* Terminal differentiation of human breast cancer through PPAR gamma. *Mol Cell* 1998; **3**:465–470.

29 Chawla A, Barak Y, Nagy L, Liao D, Tontonoz P, Evans RM. PPAR-gamma dependent and independent effects on macrophage-gene expression in lipid metabolism and inflammation. *Nat Med* 2001; **7**:48–52.

30 Rossi A, Kapahi P, Natoli G, Takahashi T, Chen Y, Karim M, *et al.* Anti-inflammatory cyclopentenone prostaglandins are direct inhibitors of IkappaB kinase. *Nature* 2000; **403**:103–108.

31 Cernuda-Morollon E, Pineda-Molina E, Canada FJ, Perez-Sala D. 15-Deoxy-Delta 12,14-prostaglandin J2 inhibition of NF-kappaB-DNA binding through covalent modification of the p50 subunit. *J Biol Chem* 2001; **276**:35530–35536.

32 Grommes C, Landreth GE, Heneka MT. Antineoplastic effects of peroxisome proliferator-activated receptor gamma agonists. *Lancet Oncol* 2004; **5**:419–429.

33 Tsubouchi Y, Sano H, Kawahito Y, Mukai S, Yamada R, Kohno M, *et al.* Inhibition of human lung cancer cell growth by the peroxisome proliferator-activated receptor-gamma agonists through induction of apoptosis. *Biochem Biophys Res Commun* 2000; **270**:400–405.

34 Bishop-Bailey D, Hla T. Endothelial cell apoptosis induced by the peroxisome proliferator-activated receptor (PPAR) ligand 15-deoxy-$\Delta^{12,14}$-prostaglandin J_2. *J Biol Chem* 1999; **274**:17042–17048.

35 Clay CE, Monjazeb A, Thorburn J, Chilton FH, High KP. 15-Deoxy-$\Delta^{12,14}$-prostaglandin J_2-induced apoptosis does not require PPAR-γ in breast cancer cells. *J Lipid Res* 2002; **43**:1818–1828.

36 Ward C, Dransfield I, Murray J, Farrow SN, Haslett C, Rossi AG. Prostaglandin D_2 and its metabolites induce caspase-dependent granulocyte apoptosis that is mediated via inhibition of IκBα degradation using a peroxisome proliferator-activated receptor-γ-independent mechanism. *J Immunol* 2002; **168**:6232–6243.

37 Chintharlapalli S, Smith R III, Samudio I, Zhang W, Safe S. 1,1-Bis(3′-indolyl)-1-(*p*-substitutedphenyl)methanes induce peroxisome proliferator-activated receptor gamma-mediated growth inhibition, transactivation, and differentiation markers in colon cancer cells. *Cancer Res* 2004; **64**:5994–6001.

38 Qin C, Burghardt R, Smith R, Wormke M, Stewart J, Safe S. Peroxisome proliferator-activated receptor gamma agonists induce proteasome-dependent degradation of cyclin D1 and estrogen receptor alpha in MCF-7 breast cancer cells. *Cancer Res* 2003; **63**:958–964.

39 Chattopadhyay N, Singh DP, Heese O, Godbole M, Sinohara T, Black PM, *et al.* Expression of peroxisome proliferator-activated receptors (PPARS) in human astrocytic cells: PPARgamma agonists as inducers of apoptosis. *J Neurosci Res* 2000; **61**:67–74.

40 Toyoda M, Takagi H, Horiguchi N, Kakizaki S, Sato K, Takayama H, *et al.* A ligand for peroxisome proliferator activated receptor gamma inhibits cell growth and induces apoptosis in human liver cancer cells. *Gut* 2002; **50**:563–567.

41 Zander T, Kraus JA, Grommes C. Induction of apoptosis in human and rat glioma by agonists of the nuclear receptor PPARgamma. *J Neurochem* 2002; **81**:1052–1060.

42 Fournier DB, Gordon GB. COX-2 and colon cancer: potential targets for chemoprevention. *J Cell Biochem Suppl* 2000; **34**:97–102.

43 Ferraro E, Corvaro M, Cecconi F. Physiological and pathological roles of Apaf1 and the apoptosome. *J Cell Mol Med* 2003; **7**:21–34.

44 Itami A, Watanabe G, Shimada Y, Hashimoto Y, Kawamura J, Kato M, *et al.* Ligands for peroxisome proliferator-activated receptor gamma inhibit growth of pancreatic cancers both *in vitro* and *in vivo*. *Int J Cancer* 2001; **94**:370–376.

45 Yin F, Wakino S, Liu Z, Hseuh HA, Collins RA, Van Herle AJ, *et al.* Troglitazone inhibits growth of MCF-7 breast carcinoma cells by targeting G_1 cell cycle regulators. *Biochem Biophys Res Commun* 2001; **286**:916–922.

46 Koga H, Sakisaka S, Harada M, Takagi T, Hanada S, Taniguchi E, *et al.* Involvement of $p21^{WAF1/Cip1}$, $p27^{Kip1}$, and $p18^{INK4c}$ in troglitazone-induced cell-cycle arrest in human hepatoma cell lines. *Hepatology* 2001; **33**:1087–1097.

47 Wang C, Fu M, D'Amico M, Albenece C, Zhou ZN, Brown lee N, *et al.* Inhibition of cellular proliferation through IkappaB kinase-independent and peroxisome proliferator-activated receptor gamma-dependent repression of cyclin D1. *Mol Cell Biol* 2001; **21**:3057–3070.

48 Castrillo A, Diaz MJ, Hortelano S. Inhibition of IkappaB kinase and IkappaB phosphorylation by 15-deoxy-$\Delta^{12,14}$-prostaglandin J_2 in activated murine macrophages. *Mol Cell Biol* 2000; **20**:1692–1698.

49 Chintharlapalli S, Papineni S, Konopleva M, Andreef M, Samudio I, Safe S. 2-Cyano-3,12-dioxylean-1,9-dien-28-ioc acid and related compounds inhibit growth of colon cancer cells through PPAR-γ dependent and independent pathways. *Mol Pharmacol* 2005; **68**:119–128.